

DESIGN AND OPTIMIZATION OF A TRANSONIC NATURAL LAMINAR FLOW AIRFOIL

U.CELLA¹, D.QUAGLIARELLA², R.DONELLI²

¹*Piaggio Aero Industries, Via Campi Flegrei 34, 80078 Pozzuoli (NA), Italy*

²*Centro Italiano Ricerche Aerospaziali (CIRA), Via Maiorise, 81043 Capua, Italy*

ABSTRACT

The design process of a transonic natural laminar flow airfoil of a swept wing is here described. An optimization procedure has been set up coupling a multiobjective genetic algorithm to a “quasi 3D” aerodynamic analysis approach. Particular attention has been devoted to the development and validation of fast and reliable numerical tools to evaluate separation and transition in presence of three-dimensional effects. The procedure has then been applied to the design of a laminar airfoil to be used in the design of a transonic wing suitable for business jet aircrafts applications.

1 INTRODUCTION

During the past decades, several European research programs have been addressed to investigate the applicability of laminar flow technology to modern transport aircrafts. The attention has been, mainly, focused on the stability of natural flow around swept wings with a leading edge sweep angle higher than 20 degrees, and with Reynolds numbers ranging between 18 and 22 millions. These projects have shown the large benefits deriving from the application of the laminar flow technology, like a substantial drag saving and consequently fuel consumption and pollution reduction. Nevertheless they have also evidenced problems like the strong sensitivity of the laminar flow to the leading edge sweep angle, to the environment conditions and the fast degradation of the aerodynamics wing performances in off-design condition. As consequence, no modern transport aircrafts, up to now, make use of the natural laminar flow technology. The studies have shown that a design of a natural laminar transonic wing with pronounced leading edge sweep angle and high Reynolds number is not possible, at the moment. Active flow control techniques, like suction are necessary. These techniques seem to work, but there are technological problems for their industrial application that are insurmountable so far. Nevertheless, transonic natural laminar wing with moderate leading edge sweep angles and lower Reynolds numbers, seems to be an achievable objective, especially improving the design methodology. In this paper, the design process of a transonic natural laminar flow airfoil for a wing of a business aircraft is described. Great attention has been devoted to the development and validation of fast and reliable numerical tools to evaluate separation and transition (Database method) in presence of three-dimensional effects. In particular, the 2.5D design methodology used to design the wing section and able to take in to account the effects of the leading edge sweep angle on the transition is described.

2 DESIGN METHODOLOGY

The successful design of a transonic NLF airfoil requires the availability of several analysis codes. Beyond an accurate aerodynamic analysis tool, a reliable prediction of the transition location is essential. To this end the method adopted should consider all the possible instability mechanisms that can develop in the flow field considered. In case of a two-dimensional design, the Tollmien-Schlichting instability scenario is the dominant. When the design process is

coupled with an optimization criterion, several codes integrated in the loop, must also fulfill high robustness and low computational cost requirements. Similar methods has been in the past successfully integrated and coupled with optimization criteria, evidencing high efficiency in two-dimensional applications (see [1] and [2]). The purpose of the present work is to extend the available methodology to the design of a NLF airfoil for a transonic swept back wing. To accomplish this task particular attention has been devoted to the appropriate modeling of the “three-dimensionality” of the boundary layer and to the evaluation of the Crossflow instability propagation mechanism, which becomes relevant increasing the sweep angle. A significant part of the study was dedicated to the selection and development of appropriate numerical tools, to acquire confidence of their limit and capabilities, and to integrate them in an efficient manner in a multiobjective optimization loop based on genetic algorithms.

2.1 Optimization

Genetic algorithms (GAs) are becoming widely used in the solution of several engineering design problems. Indeed, their robustness and flexibility are clear advantages with respect to other more traditional approaches. In particular, the growing need of a multidisciplinary and integrated approach to the design process produced an increasing interest towards the use of genetic algorithms as an optimization technique that allows an easy and direct implementation of multiobjective optimization.

Most real-life design procedures are complex tasks that have to deal with multidisciplinary environments, not always clearly defined targets, and constraints to be satisfied. The optimization process must consider several different and usually conflicting objectives, and the best compromise level obtainable might not be prioristically known. The possibility of looking not only for a single good solution but for a set of solutions (the Pareto set) that satisfies different levels of compromise might be of great help to the decision maker that must select the most suitable one (see [3, 4, 5, 6]).

Indeed, when conflicting requirements have to be satisfied at the same time, the traditional approach is to reduce the multiobjective problem into a classical single objective one either through a weighted combination of the objective functions or by introducing a set of supplementary constraints. In this way, one solution is found representing a compromise between the different requirements. The drawback of this approach is that the solution depends on the arbitrary choice of weights or constraints. From this point of view, the capability of genetic algorithms of allowing a direct and efficient implementation of multiobjective optimization, where a given set of objective functions are optimized without the need of being arbitrarily combined, appears as a more straightforward approach, and it is a substantial improvement with respect to traditional techniques.

Furthermore, two other issues make genetic algorithms more than attractive and maybe unique among the aerodynamic design optimization methods: they are usually much more robust than gradient based algorithm and can tolerate even approximate or noisy design objectives evaluation; they can be efficiently parallelized and can therefore take full advantage of massively parallel computer architectures.

Besides a large number of examples of engineering application that can be found in the literature there is also a growing interest and attention of the scientific community towards evolutionary multiobjective optimization, as outlined in [7].

2.1.1 Optimization and design concepts

The optimization system is an automatic procedure that starts from a given aeronautical configuration and looks for an improved one. In order to do that, *design variables*, which can measure the modification with respect to the given configuration, and an *objective* function, which allows to measure the improvement of the configuration, must be defined.

From a theoretical point of view, the design variables represent the coordinates of a point in a sub-set of the real space in N dimensions \mathbb{R}^N , where N is the number of design variables. It is assumed that an aeronautic configuration can be associated to each point of such a set, and an objective function can be evaluated for each configuration. With this assumption, a correspondence exists between the space of the design variables and the objective function, and points can be located, which correspond to the absolute minimum of the objective. The configuration(s) which is (are) associated to the minimum of the objective function is called *optimum*.

Constraint functions can also be defined and evaluated, like the objective; by convention those points of the design variables space, which correspond to positive values of at least one constraint function, are taken out of the set.

Our optimization system is based on three main procedures: the optimizer, the configuration generator, and the objective and constraint functions evaluator.

From the mathematical point of view, the optimizer is an algorithm that looks for the absolute minimum of a function, which is defined in a sub-set of \mathbb{R}^N . When this function is continuous, together with its first derivatives, gradient-based optimization algorithms can be adopted. In case that no information is available concerning the derivatives of the objective, or in case that the definition domain is multi-connected, then a genetic algorithm is more appropriated.

Constraint functions can restrict the searching region, by setting boundaries inside the domain, and in this way they can help the optimizer (particularly when a gradient-based method is adopted, which is capable to locate and follow the boundaries); on the other hand, boundaries could also dissect the definition domain, creating a multi-connected region, which cannot be handled anymore by a gradient-based optimization method.

When the values of the design variables are modified, the modifications are reflected to some of the physical parameters which define the aeronautic configuration. Links between physical parameters and design variables are set in the phase preliminary to the optimization, named *Problem Definition*. The configuration is defined by the design variables and the input *reference* configuration (the usual convention is to consider as *reference* that configuration corresponding to design variables all equal to 0): for each configuration a unique value of the objective and constraint functions must exist. The configuration generator produces all the information required to execute the evaluation procedure.

During the evaluation procedure the configuration is analyzed, in order to compute the objective function and the constraints. For aerodynamic analysis a grid generator and a CFD solver are required, together with tools for post-processing the solver output data. Geometric analysis could also be required (for example to compute airfoil thickness and to rescale it to a given value).

Each operational condition that has to be considered to evaluate the objective and constraint functions is called *design point*. When more operational conditions must be taken into account to evaluate the objective and the constraints, then we are performing a *multi-point* optimization.

Multi-point optimization can be performed in two substantially different ways. The first one combines each design point in a single objective function using different weights related to the importance given to each design point. Another approach is *multiobjective* optimization [8, 9] where several objective functions can be considered by introducing a ranking criteria so that the configurations can be classified into dominated and non-dominated.

2.1.2 The multiobjective genetic algorithm

The multiple objective genetic algorithm used here is described in [1, 2]. The definition of optimality for multiobjective optimization problems is here reported for the sake of completeness, while more details about multiobjective problems properties can be found in [9, 10].

The main difference between single and multiple objective optimization is the definition of optimal solution, that is an extension of the single objective optimum concept.

A feasible solution to a multiobjective optimization problem is said optimal, or non dominated, if, starting from that point in the design space, the value of any of the objective functions cannot be improved without deteriorating at least one of the others.

This is translated in mathematical terms by introducing the notion of domination for two real-valued vectors of n elements: $\mathbf{f} = (f_1, \dots, f_n)$ is partially less than $\mathbf{g} = (g_1, \dots, g_n)$ (in symbols $\mathbf{f} <_p \mathbf{g}$) if:

$$\forall i \in (1, \dots, n) f_i \leq g_i \quad \text{and} \quad \exists i : f_i < g_i \quad (1)$$

If $\mathbf{f} <_p \mathbf{g}$, we say that \mathbf{f} dominates \mathbf{g} . Consequently, a feasible solution \mathbf{x}^* is said a Pareto optimal if and only if it does not exist another feasible solution \mathbf{x} such that $\mathbf{f}(\mathbf{x}) <_p \mathbf{f}(\mathbf{x}^*)$.

In general, the optimal solution to a multiobjective problem is not unique. All feasible solutions can, indeed, be classified into dominated and non-dominated (Pareto optimal) solutions, and the set of non-dominated solution is called Pareto front. Solving a multiobjective optimization problem means, therefore, to find this set or to approximate it with a representative subset. Afterwards the decision-maker's preference may be applied to choose the best compromise solution from the generated set.

A genetic algorithm can directly use the above defined dominance criteria to select elements appointed for reproduction and, hence, to drive the evolution of the population towards the Pareto front [8].

The selection operator used here is random walk. The locally non-dominated population elements met in the walk are selected for reproduction. If more non-dominated solutions are met, then the first one encountered is selected. At the end of every new generation, the set of Pareto optimal solutions is updated and stored.

A sort of extension of the elitism strategy to multiobjective optimization is obtained by randomly selecting an assigned percentage of parents from the current set of non dominated solutions.

2.1.3 Airfoil shape parametrization

The airfoil shape is defined as a linear combination of an initial geometry $y_0(x)$ and some modification functions, $f_i(x), i = 1, \dots, n$:

$$y(x) = k \left(y_0(x) + \sum_{i=1}^n w_i f_i(x) \right) \quad (2)$$

where w_i are the design variables and k is a free parameter that can be used to scale the airfoil to a given thickness. Here the classical Hicks-Henne, Legendre, Wagner rear-loading and polynomial functions are used.

2.2 Physics modeling

The airfoil performances are evaluated by a number of steps synthesized in the first loop of the design flowchart, marked by the dotted block named “ANALYSIS” (fig 1). Three methods are integrated to compute the characteristics of the selected geometry: a boundary layer code able to compute the three-dimensional velocity profiles of a swept wing section, a stability analysis method able to estimate the transition location in presence of crossflow contamination and a two-dimensional Euler/Thin Layer code that performs the aerodynamic analysis of the airfoil and provides the input pressure distribution for the 3D BL code.

In each cycle of the loop, the C_p is recomputed and the transition locations updated until the pressure distribution converges to a constant value.

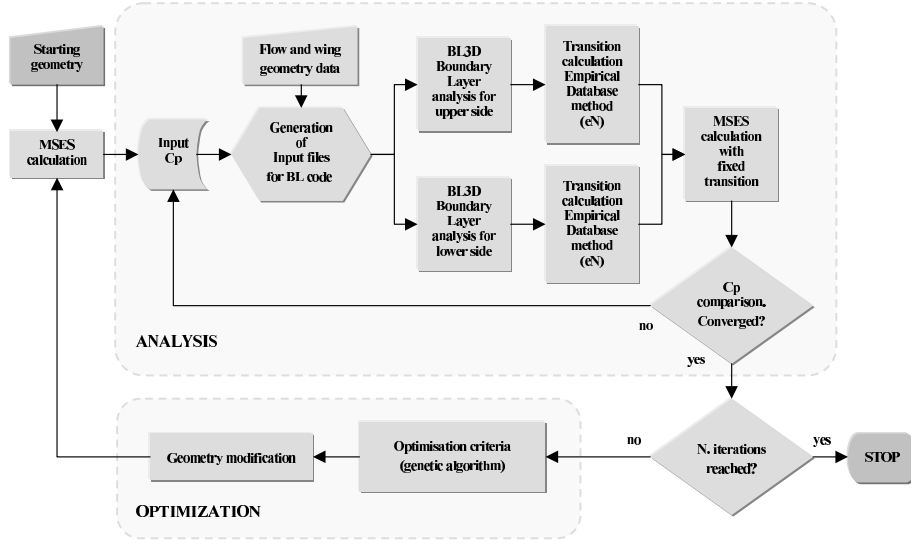


Figure 1: Optimization work flow.

2.2.1 Aerodynamic tools

The aerodynamic analysis is performed by the MSES code. It provides a very fast and reasonably accurate two-dimensional solution solving the Euler equations in the non viscous field and the integral form of the boundary layer equations near the wall [11]. Small separation regions are modeled giving an accurate solution in case of small bubbles or moderate separations but reducing the validity of the solution when larger separation phenomena appears. It can also perform a simplified stability analysis for the Tollmien-Schlichting transition estimation using the e^N envelope semi-empirical transition criterion. In this work, in addition to the MSES criterion, the transition location is externally calculated by the Database method and imposed in the calculation to take into account the crossflow instabilities of swept wings.

In order to use a two-dimensional tool (as MSES is) to perform the analysis of a three-dimensional swept wing section, a plane section in which the values of the orthogonal gradients are minimal has to be individuated. Such airfoil and its aerodynamic characteristics is computed referring to the so called “principle of cosine” [12]. More in detail, once the target geometry (thickness, leading edge radius, trailing edge thickness) and aerodynamic constraints (Mach, Reynolds, lift and pitching moment coefficient) regarding the streamflow section of the wing have been defined, the principle of cosine is applied in order to derive the corresponding two-dimensional targets and constraints. This rule refers to infinite swept wings with low angle of incidence but it maintains its validity in case of finite wings with high aspect ratio. The following formulas are used to derive the corresponding 2D parameters:

$$\left(\frac{t}{c}\right)_{2D} = \frac{t}{c} \cdot \frac{1}{\cos \Lambda}; \quad C_{l_{2D}} = \frac{C_l}{\cos^2 \Lambda}; \quad Re_{2D} = Re \cos^2 \Lambda; \quad Mach_{2D} = Mach \cos \Lambda \quad (3)$$

where Λ is the wing sweep angle ¹

¹The airfoil commonly considered for a better two-dimensional approximation of a swept tapered wing is the section with the plane orthogonal

2.2.2 Boundary layer solution

Once obtained the pressure distribution from the aerodynamic code, a manipulation of its solution is necessary in order to create a valid input file format for the boundary layer solver. In particular the stagnation point needs to be found and two different input files, respectively for upper and lower surface analysis, must be created.

The boundary layer analysis is performed by the BL3d code based on the conical flow approach, also known as Kaups-Cebeci approach. Its method is based on the simplifying conical flow assumption valid for trapezoidal planform wing geometry without pressure gradient along the generators. The wing is modeled as a cone (the twist is neglected) whose generators pass through the provided airfoil geometry. The root and the tip airfoil are similar and simply scaled. The boundary layer equations are written in conical coordinates and solved along the arc obtained from the intersection with a sphere whose center is the origin of the wing generators. This approximation permits to obtain a three dimensional solution of the boundary layer of swept tapered wing, in a form similar to two-dimensional boundary layer equations [13].

2.2.3 Stability analysis

Starting from the boundary layer solution, a stability analysis is performed on each side of the airfoil in order to estimate the transition location. The stability solution is obtained using the Database method. Such a method is based on an analytical representations of the disturbances growth rate as a function of some relevant boundary layer parameters [14]. These analytical representations have been obtained by an accurate investigation on the growth rates of the disturbances computed using methods based on the linear stability theory for a particular well known airfoil.

It has been shown that for a two dimensional boundary layer, the stability properties of a flow (growth rate amplification, transition, by-pass, etc.), are strictly connected to the Reynolds number, to the frequencies and to the shape of the boundary layer velocity profiles. The database method is based on the idea of computing the stability properties of a test case and to find analytical correlations that can be applied to any other self similar real situations. The final task is to estimate the evolution of the N factor along all stations of the airfoil for both Tollmien-Schlichting and crossflow waves [15].

Database usage Using as input the 3D boundary layer solution of a generic airfoil, the code computes the N factor for a set of frequencies and direction close to the streamlines (Tollmien-Schlichting instability) and for a set of directions close to 90° at frequency close to zero and individuates the envelope of the maximum values for N_{TS} and N_{CF} . The envelope of the N curves for all frequencies and direction, provides the more general N factor distribution (“*envelop of envelop*” method) that takes into consideration all the possible combination of disturbances. This method is the one used in this work.

The choice of the critical N factor to be used constitutes the main limit of the criterion and it must be estimated by experimental observation. In this paper a conservative approach has been adopted choosing a value of 8 as critical N factor.

The calculated transition location is imposed in the following cycle of aerodynamic analysis and the loop continues until the pressure distribution does not change anymore.

3 DESCRIPTION OF THE DESIGN TARGET

The choice of the characteristic airfoil target performances refer to the wing designed for a medium size business jet aircraft class. It is a tapered swept back wing with a sweep angle of 20° at the leading edge. The selected airfoil is the streamwise section at the 50% of the exposed semispan. From a preliminary evaluation, four design conditions with the relatives constraints have been defined: one is referred to the climb condition, two to the cruising Mach number and one to the high speed cruise. The selection of the second point at cruising speed has been done in order to define a polar laminar bucket. Table 1 summarizes the four target design points and table 2 the geometric constraints.

Laminar airfoils are known to have a dangerous degradation of performance at low speed. Therefore particular attention must be paid to the high lift requirements and stall type characteristics of the designed profile. For such a reason a constraint in the leading edge radius has been imposed.

to the sweep angle at the 25% of the chord. In this work, on the contrary, the airfoil optimized is the one corresponding to the section with the plane orthogonal to the leading edge of the wing. This choice is justified by the necessity of having high accuracy in the region where the development of Crossflow instabilities is higher.

<i>Design point</i>	<i>Mach</i>	<i>Reynolds</i>	C_l	C_m
Climb	0.7	8 millions	0.63	-
Cruise 1	0.75	8 millions	0.55	> -0.11
Cruise 2	0.75	8 millions	0.4	> -0.11
High speed	0.78	8 millions	0.5	> -0.13

Table 1: *Aerodynamic targets of the airfoil.*

Maximum thickness	0.124c
Thickness at $x/c = 0.85$	0.04c
Trailing edge thickness	0.002c
Leading edge radius	0.011c
Single sign curvature region	$0.15 < x/c < 0.6$

Table 2: *Geometric constraints of the airfoil.*

4 OPTIMIZATION STRATEGY

In most of cases the required airfoil performances must satisfy several design conditions. The choice of a multiobjective optimization strategy seems then to be natural. This approach, however, involves a sensible increase in the complexity of the calculation setup and the selection of the compromising solution can be very difficult. The number of the optimization objectives should then be reduced to the minimum in order to reasonably limit the complexity of the calculation. Furthermore, an efficient optimization strategy requires the imposition of realistic constraints and an appropriate selection of the design targets. For this reason a significant part of the study has been dedicated to the research of an efficient optimization strategy and to the proper selection of the design constraints. The design process, in fact, passed through the setup of a number of optimization loops whose objective was to individuate the design limits, the margins of improvement and the constraints selection for a final optimization loop.

4.1 The reference airfoil

The selection of the starting geometry seems in general to play an important role in an optimization process, at least to speedup the convergence to the “optimum” solution. In this work the ELFIN geometry has been adopted as reference starting solution.

The ELFIN I and II European research project had the objective of developing and assessing numerical tools for boundary layer investigation and transition prediction methods. Within this project, a Natural Laminar Flow airfoil has been designed with the aim to setup a test case for in-flight laminar flow measurements. A NLF glove was built and mounted on the center part of a Fokker 100 wing.

The ELFIN design was developed with the objective to obtain 50% of laminar flow on a swept wing (20° at the leading edge) at a Reynolds number of 22 millions, $Mach = 0.75$ and $C_l = 0.4$. To reach this target, the project had to develop a very stable region on the first part of the airfoil surface. The lower Reynolds number of our case suggests the possibility of performance improvement in the design.

4.2 Procedure adopted

The design procedure started from the setup of a first single objective optimization. Several loops followed and each solution was used as starting geometry of the following cycle. The information collected during this process gave the indication of the opportune configuration of the final optimization loop. In all the loops the geometric constraints reported in the table 2 (scaled by the principle of cosine) were imposed.

4.2.1 Preliminary optimization cycles

Loop 1 A single objective optimization was first setup. The design point is referred to the freestream cruise 1 condition reported in the table 1: $Mach = 0.75$ and $C_l = 0.55$. The corresponding 2D scaled values are: $Mach = 0.705$ and $C_l = 0.6229$. The transition was kept free in MSES on both sides of the airfoil.

The laminar flow on the resulting geometry exceeded the 60% of surface on both sides of the airfoil. Zero wave drag was also obtained, hence, a minimum possible value of drag was reached.

The figure 2 reports the pressure distribution of the optimized airfoil.

Loop 2 The same optimization configuration as the previous run was setup but imposing a fixed transition at 60% of the chord on the upper side of the airfoil. The intention was to verify if an external limitation in the laminar flow extension could increase the margins of stability of the boundary layer but the result of the optimization indicated an opposite trend. In the following calculations the transition was always kept free when no wave drag was present.

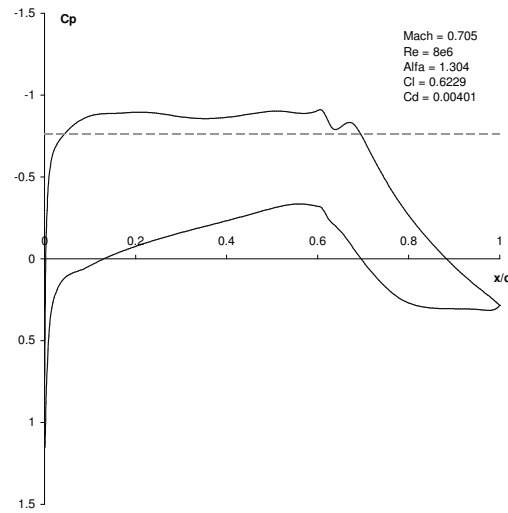


Figure 2: *C_p distribution of the first loop solution.*

Loop 3 Once the design point and the subsequent optimization configuration to reach the minimum possible drag in cruising condition were defined, the optimization in high speed condition was considered. A two objective drag minimization was setup at the two following conditions:

- **Objective 1:** Mach = 0.75 (Mach_{2D} = 0.705), C_l = 0.55 (C_{l2D} = 0.6229), free transition.
- **Objective 2:** Mach = 0.79 (Mach_{2D} = 0.742), C_l = 0.5 (C_{l2D} = 0.5662), free transition.

The Mach number of the second objective is imposed slightly higher than the high speed design condition in order to test the optimization of the wave drag. The figure 3 reports the drag of the five more representative solution of the Pareto frontier obtained (curve marked by +). In the same graph the solution obtained from the analysis of the selected geometries imposing the transition at 50% of the chord is plotted.

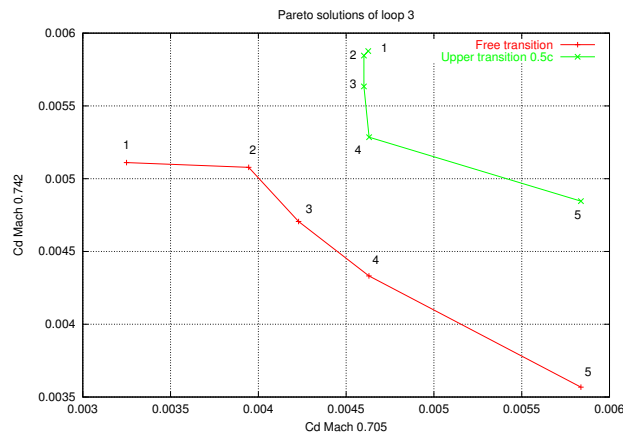


Figure 3: *Pareto frontiers of the third optimization loop.*

The solution number 1 is more oriented to have high performance at the objective 1 conditions (Mach = 0.75) rather the airfoil number 5 has better performance at Mach = 0.79. The Pareto curve obtained imposing the transition indicates that all the airfoils, except the number 5, have almost the same drag at Mach = 0.75. The choice of the solution number 4 seems then to be the optimum compromise. However, a more conservative approach might suggest to require a higher stability margin of the laminar boundary layer. In such a case, it may be opportune to sacrifice few drag counts at high speed in order to have a more stable boundary layer in cruising condition, and hence, to choose the solution number 1.

Loop 4 The stability analysis of the solutions obtained in the previous optimization loop at high speed conditions, evidenced that in most of cases the boundary layer is very stable up to the 70% on the upper side and up to the 60% on the lower. The drag of the airfoil is on the contrary influenced by the presence of a significant wave drag component.

In order to orient the optimization more towards the reduction of the wave component, the fourth optimization loop has been setup with a similar configuration as the previous one but fixing the transition on the upper side for the objective 2.

- **Objective 1:** Mach = 0.75 (Mach_{2D} = 0.705), C_l = 0.55 (C_{l2D} = 0.6229), free transition.
- **Objective 2:** Mach = 0.78 (Mach_{2D} = 0.733), C_l = 0.5 (C_{l2D} = 0.5662), upper transition at 0.6c.

The compromise geometry selected from the Pareto frontier obtained was checked in climb condition (figure 4). The stability curve evidenced a significant reduction of laminar flow on the upper surface.

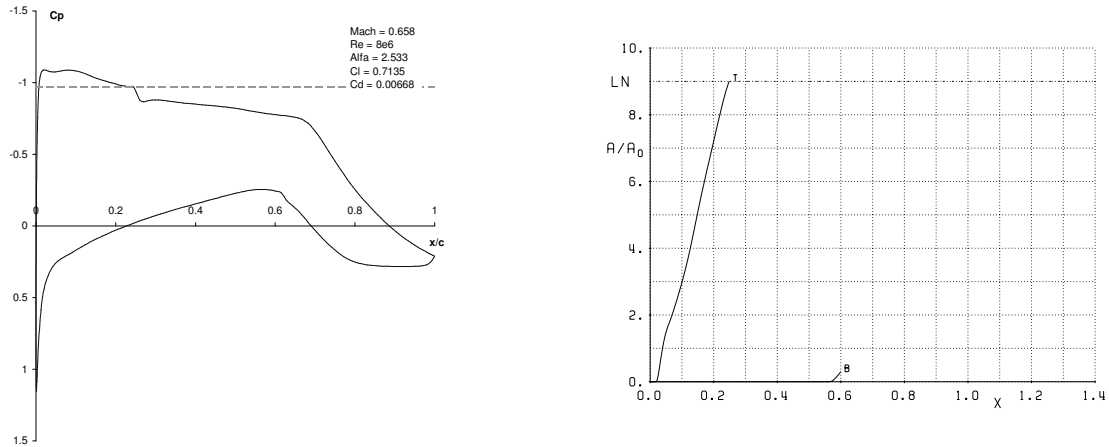


Figure 4: Climb performance of selected loop 4 solution.

Loop 5 The climb requirement of the design has been taken into account in the next multiobjective optimization. The second design objective is the high speed condition.

- **Objective 1:** Mach = 0.7 (Mach_{2D} = 0.658), C_l = 0.63 (C_{l2D} = 0.7135), free transition.
- **Objective 2:** Mach = 0.78 (Mach_{2D} = 0.733), C_l = 0.5 (C_{l2D} = 0.5662), upper transition at 0.6c.

The two conditions were efficiently optimized but all the solutions evidenced a significant degradation of boundary layer stability at cruising speed (Mach = 0.75).

Loop 6 The need of taking into account more design targets begins here to be considered. It is still a two objective configuration but the second point is a combination of the design points in climb and fast cruising speed with different weight.

- **Objective 1:**
 - Weight = 1, Mach = 0.75 (Mach_{2D} = 0.705), C_l = 0.55 (C_{l2D} = 0.6229), free transition.
- **Objective 2:**
 - Weight = 2, Mach = 0.7 (Mach_{2D} = 0.658), C_l = 0.63 (C_{l2D} = 0.7135), free transition.
 - Weight = 1, Mach = 0.78 (Mach_{2D} = 0.733), C_l = 0.5 (C_{l2D} = 0.5662), upper transition at 0.6c.

Excellent climb and cruising performance was obtained from the Pareto solutions. The choice of the objective weight was however not opportune since a great increment in wave drag in high speed (Mach = 0.78) was evidenced. Furthermore, it was evaluated that the optimization of a geometry for climb condition involves an excessive increasing in moment coefficient at cruising speed.

Loop 7 This last preliminary optimization loop was setup with the intention to consider all the design points and to evaluate the limit of an optimum compromise that take into consideration all the design issues emerged so far. The lower limit of the laminar bucket of the cruising polar is, for the first time, an optimization objective.

A four-objective optimization has been setup with the following configuration:

- **Objective 1:** Mach = 0.7 (Mach_{2D} = 0.658), C_l = 0.63 (C_{l2D} = 0.7135), C_m > -0.11, free trans.
- **Objective 2:** Mach = 0.75 (Mach_{2D} = 0.705), C_l = 0.55 (C_{l2D} = 0.6229), free trans.
- **Objective 3:** Mach = 0.75 (Mach_{2D} = 0.705), C_l = 0.4 (C_{l2D} = 0.453), free trans.
- **Objective 4:** Mach = 0.78 (Mach_{2D} = 0.733), C_l = 0.5 (C_{l2D} = 0.5662), upper trans. at 0.6c.

A four dimensional Pareto frontier was obtained. The processing of such a solution is very demanding and the selection of the optimum geometry is very difficult. The computation gave, however, the indication of the possible performances that the airfoil can evidence considering all the design conditions.

4.2.2 Final optimization

The analysis of the last multiobjective optimization helped to choose the reasonable target performance for the design. It was decided to setup a single objective optimization in which the target is the minimum drag in cruising condition (Mach_{2D} = 0.705 and C_{l2D} = 0.6229) and imposing as constraints the selected target drag in the other design points.

Table 3 summarizes the design constraints of the final optimization.

<i>Design point</i>	<i>Mach</i>	<i>Reynolds</i>	<i>C_l</i>	<i>C_{m,max}</i>	<i>C_{d2D,min}</i>	<i>N_{cr}</i>	<i>Transition</i>
Climb	0.7	8 millions	0.63	-	55 dc	8	Free
Cruise 1	0.75	8 millions	0.55	-0.11	-	8	Free
Cruise 2	0.75	8 millions	0.4	-0.11	40 dc	8	Free
Fast cruise	0.78	8 millions	0.5	-0.13	55 dc	8	Fixed 0.6c up

Table 3: *Design constraints of the final optimization cycle.*

The computation result is an airfoil that satisfies several requirements and takes into account also a certain margin of stability in cruising condition.

4.3 Design refinement

The final optimized geometry evidenced small irregularities in the upper pressure distribution and a pressure peak on the lower side. The lower peak in particular is responsible of a premature destabilization of the boundary layer, causing a sudden destroy of the laminar flow at low angle of incidence. In order to reduce this effects an accurate manual refinement of both the pressure distribution and geometry has been done. The pressure distribution was smoothed by CAD and a new geometry was obtained using an inverse method. The lower geometry close to the leading edge was slightly modified in order to reduce the pressure peak.

The new airfoil was verified in all the design points and only a slight degradation of performance (in the order of a drag count) was evaluated. The pressure distribution with free transition and the MSES stability curves² of both the optimized and the smoothed airfoil is reported in figure 5.

Table 4 compares the performances of the smoothed airfoil in the four design conditions with the starting reference geometry (ELFIN design). The drag values are calculated with MSES fixing the transition at 60% of the chord on both sides.

<i>Design point</i>	<i>Starting airfoil</i>	<i>Final design</i>
Climb: Mach = 0.7 (Mach _{2D} = 0.658), C _l = 0.63 (C _{l2D} = 0.7135)	79.8 dc	74.7 dc
Cruise 1: Mach = 0.75 (Mach _{2D} = 0.705), C _l = 0.55 (C _{l2D} = 0.6229)	38.6 dc	39.2 dc
Cruise 2: Mach = 0.75 (Mach _{2D} = 0.705), C _l = 0.4 (C _{l2D} = 0.453)	50.4 dc	38.6 dc
Fast cruise: Mach = 0.78 (Mach _{2D} = 0.733), C _l = 0.5 (C _{l2D} = 0.5662)	67.5 dc	52.1 dc

Table 4: *Performances of the design compared to the starting geometry.*

²The MSES transition criterion is always active. Whatever criterion is first satisfied (MSES or Database) will determine the transition location.

CONCLUSIONS

The design process and the multiobjective optimization, using genetic algorithms, of a transonic NLF airfoil of a swept wing has been presented. A significant part of the work was dedicated to the definition of the opportune optimization strategy and to the setup of an efficient computational configuration.

The target design points of the airfoil have been defined considering four flying conditions to which correspond the following design parameters:

- **Climb:** Mach = 0.7, Reynolds = $8e6$, $C_l = 0.63$.
- **Cruise 1:** Mach = 0.75, Reynolds = $8e6$, $C_l = 0.55$.
- **Cruise 2:** Mach = 0.75, Reynolds = $8e6$, $C_l = 0.4$.
- **High speed:** Mach = 0.78, Reynolds = $8e6$, $C_l = 0.5$.

The starting reference geometry was the transonic laminar glove profile designed for flying test purpose during the first ELFIN European research project and mounted on a Fokker 100 semispan wing. The target of such design was to extend the laminar flow up to the 50% of the chord at Mach 0.75, Reynolds 22 millions and 0.4 as lift coefficient.

A design procedure has been defined and an optimization tool has been developed. This tool is composed by two main part: the first integrates a two-dimensional aerodynamic analysis code (MSES) with a three-dimensional boundary layer solver (BL3d) and with a stability analysis method (Database) with a “quasi 3D” approach, the latter contains the optimization criterion and the geometry parameterizations.

Several preliminary single and multiobjective optimization loops have been setup with the aim of defining the realistic targets of the design and evidencing the possible areas of improvement. This process allowed to acquire confidence in the definition of the opportune constraints to be imposed and to drive the optimization towards the design of an airfoil with the best compromising performances in all the flying conditions.

The final design loop was a single objective optimization with a minimum drag target at the first cruising condition. The realistic performance that the final geometry could evidence in the other design points were imposed through penalties.

The optimized airfoil evidenced small irregularity in the pressure coefficient distribution. A post-design pressure manual smoothing was necessary to refine the design. A new geometry was finally obtained by inverse method and by CAD.

The resulting geometry, showed to have better performance than the starting reference airfoil. In particular a significant reduction of the compressibility drag in high speed has been obtained. An extension of laminar flow of more than 60% of the surface was also reached in all the cruising condition.

ACKNOWLEDGMENTS

Thanks are due to prof. Mark Drela for allowing the use of his MSES code in our research work.

REFERENCES

- [1] Vicini, A. and Quagliarella, D., “Inverse and Direct Airfoil Design Using a Multiobjective Genetic Algorithm,” *AIAA Journal*, Vol. 35, No. 9, Sept. 1997, pp. 1499–1505.
- [2] Vicini, A. and Quagliarella, D., “Airfoil and Wing Design Through Hybrid Optimization Strategies,” *AIAA Journal*, Vol. 37, No. 5, May 1999, pp. 634–641.
- [3] Keeney, R. L. and Raiffa, H., *Decisions With Multiple Objectives: Preferences and Value Tradeoffs*, Cambridge University Press, 1993.
- [4] Chankong, V. and Haimes, Y. Y., *Multiobjective decision making: theory and methodology*, North Holland series in system science and engineering; 8, North Holland, New York, 1983.
- [5] Zeleny, M., *Multiple Criteria Decision Making*, McGraw-Hill, New York, 1982.
- [6] Eschenauer, H., Koski, J., and Osyczka, A., *Multicriteria Design Optimisation Procedures and Applications*, Springer-Verlag, Berlin, 1990.

- [7] Coello, C. A., "Guest Editorial: Special Issue on Evolutionary Multiobjective Optimization," *IEEE Transactions on Evolutionary Computation*, Vol. 7, No. 2, April 2003, pp. 97–99.
- [8] Goldberg, D. E., *Genetic Algorithms in Search, Optimization and Machine Learning*, Addison-Wesley, Reading, Massachusetts, Jan. 1989.
- [9] Deb, K., "Multi-objective Genetic Algorithms: Problem Difficulties and Construction of Test Problems," *Evolutionary Computation*, Vol. 7, No. 3, 1999, pp. 205–230.
- [10] Quagliarella, D. and Vicini, A., "Coupling Genetic Algorithms and Gradient Based Optimization Techniques," *Genetic Algorithms and Evolution Strategies in Engineering and Computer Science*, edited by D. Quagliarella, J. Périaux, C. Poloni, and G. Winter, John Wiley & Sons Ltd., England, Nov. 1997, pp. 289–309.
- [11] Drela, M., *A User's Guide to MSES 2.9*, MIT Computational Aerospace Sciences Laboratory, October 1995.
- [12] Losito, V., *Fondamenti di Aeronautica Generale*, Accademia Aeronautica, 1991.
- [13] Kaups, K. and Cebeci, T., "Compressible Laminar Boundary Layers with Suction on Swept and Tapered Wings," Tech. rep., McDonnell Douglas corporation, September 1976.
- [14] Donelli, R. S. and Casalis, G., "Database Approach - Stationary Mode Treatment," Tech. Rep. ALTTA-CIRA-TR-AEP-01-039, CIRA and ONERA, April 2001.
- [15] Arnal, D., "Three-Dimensional Boundary Layers: Laminar-Turbulent Transition," Tech. Rep. 741, AGARD, ONERA.

APPENDIX

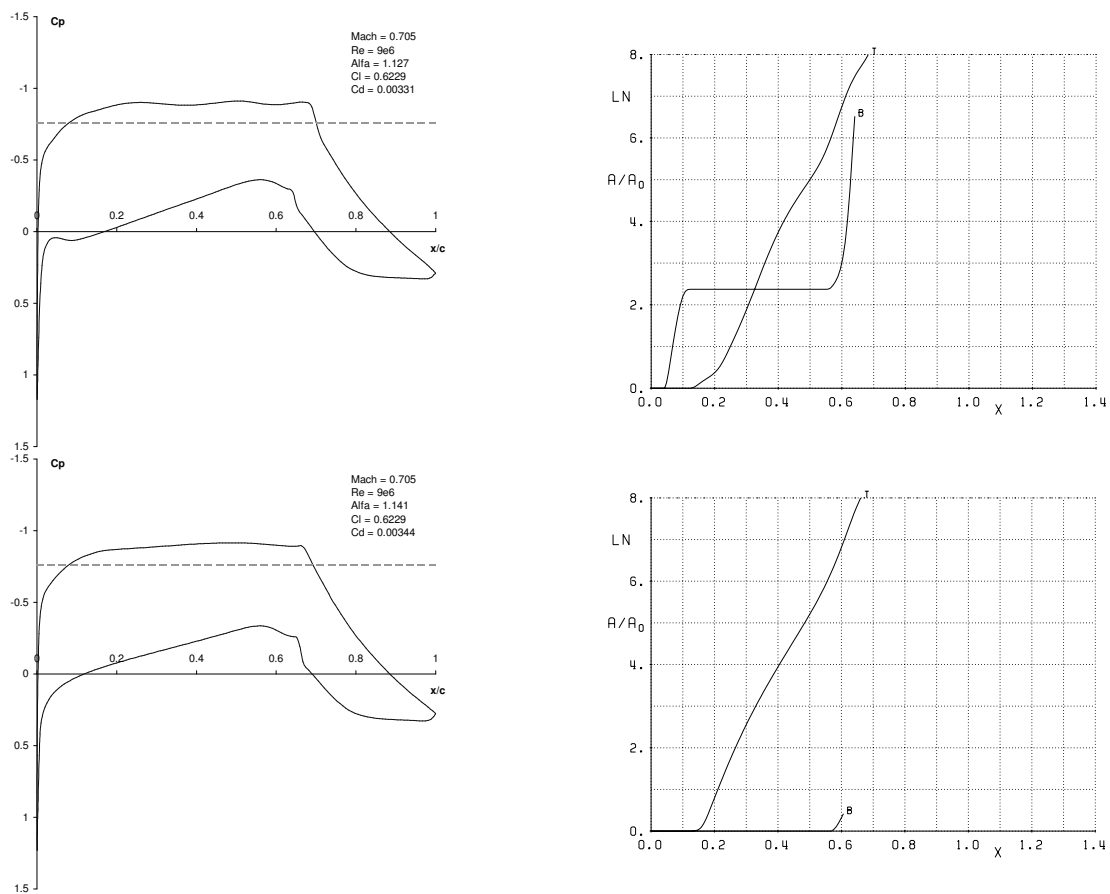


Figure 5: Pressure distribution before and after smoothing.

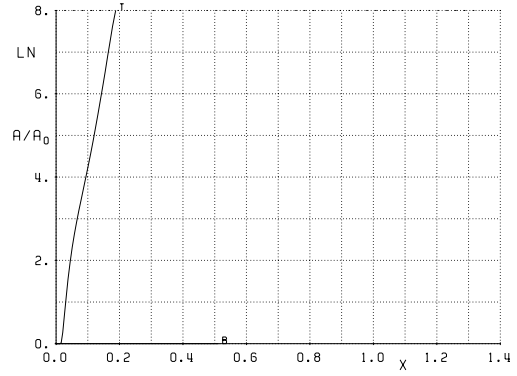
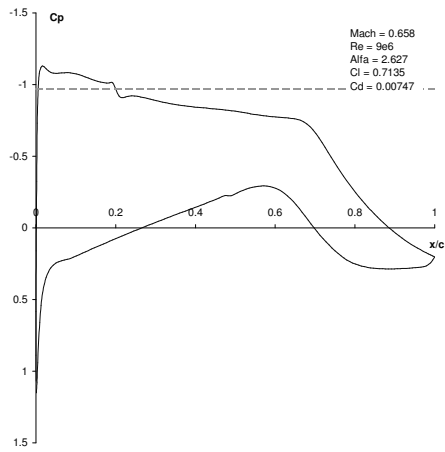


Figure 6: Final airfoil, Climb: $Mach = 0.7$, $C_l = 0.63$.

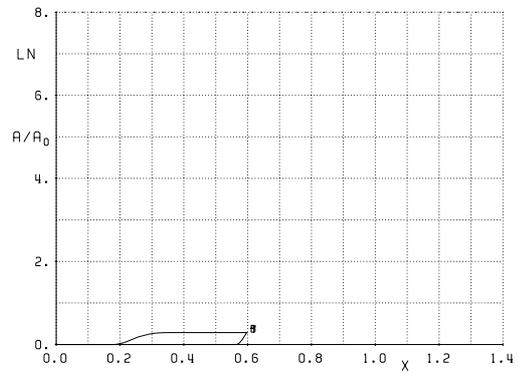
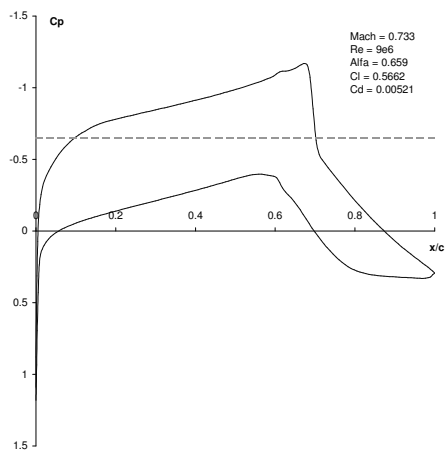


Figure 7: Final airfoil, High speed: $Mach = 0.78$, $C_l = 0.5$, transition at $0.6c$.

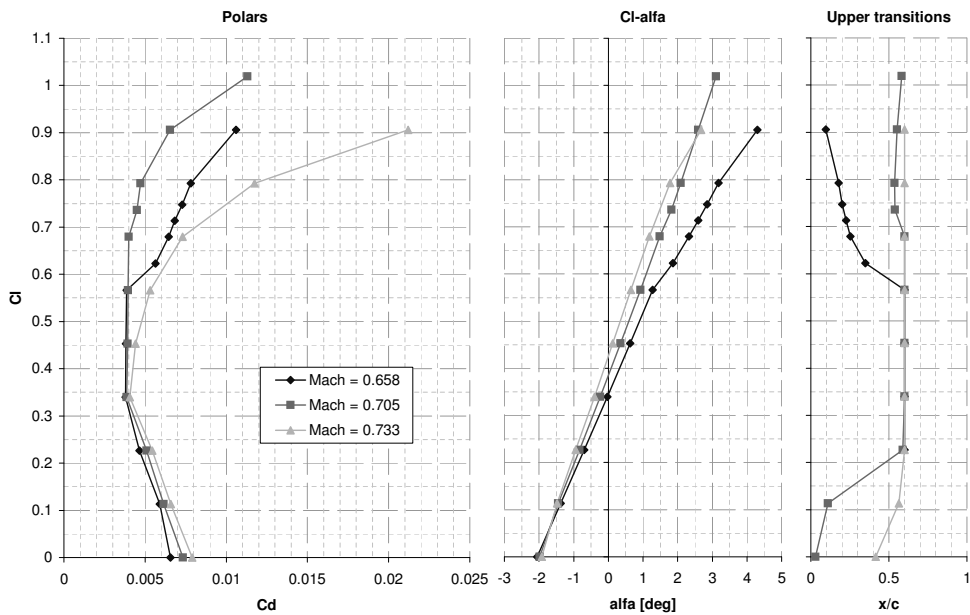


Figure 8: Polar curves of the final airfoil (MSES solution).